Fundamental Investigation of Direct Cathode Regeneration Using Chemically Delithiated Lithium Cobalt Oxides

Md. Sajibul Alam	Bhuyana and	Hosop	Shin ^{a,*}

^a Department	of Mechanical	and Energ	gy Engineering	, Indiana	University	Purdue	University	Indianapolis
Indianapolis,	IN 46202, Uni	ted States						

*Corresponding author. Tel.: +1 317-278-7305

E-mail address: shinho@iupui.edu (Hosop Shin)

Abstract

Reusing valuable cathode materials from end-of-life (EOL) Li-ion batteries can help decrease dependence on mining of raw materials for producing cathodes, while preventing commodity prices from rising. This study employed chemically delithiated cathodes that are analogous to spent cathodes but free of impurities to fundamentally elucidate the effectiveness of cathode regeneration. Two lithium cobalt oxides (LCOs) were synthesized via chemical delithiation at different degrees of delithiation. Their material and electrochemical characteristics were systematically compared before and after hydrothermal-based cathode regeneration. The material and electrochemical characteristics were further evaluated and compared with those of pristine LCO. Both LCOs, at high and low states of health (SOH), recovered their reversible capacity and cycle performance comparable to those of pristine LCO. However, the high-rate performance (2C) of the regenerated LCOs was not comparable to that of pristine LCO. The slight increase in cell resistance of the regenerated LCOs was attributed to their lower high-rate performance, which was identified as a key challenge of cathode regeneration. Our study provides valuable insights into the effectiveness of cathode regeneration by elucidating the process underlying regeneration of disordered Lideficient LCOs at different levels of SOH.

Keywords: direct recycling, cathode regeneration, Li-ion battery, end-of-life batteries, lithium cobalt oxide

1. Introduction

Lithium-ion batteries (LIBs) have gained foothold in the secondary energy storage market owing to their energy density, power output, cycle stability, and rising global production capacity. They have transformed the consumer electronics sector and sparked a global race to electrify transportation. The transportation sector is the fastest expanding contributor of greenhouse gas (GHG) emissions, leading to global warming. Sieven the increasing need to reduce carbon emissions from fossil fuels, the market for electric vehicles (EVs) has been growing rapidly. Since 2017, there have been 3 million EVs in the global market, which is expected to grow to 530 million by 2040. Thus, the number of end-of-life (EOL) LIBs retired from EVs is expected to increase dramatically over the next decade. For instance, it is estimated to generate 11.36 million waste LIBs in China by 2030; however, only 3.4 million waste LIBs are expected to be recycled through the conventional recycling route. Without new recycling capabilities to manage waste LIBs, spent LIBs containing flammable and toxic materials could harm the environment. In addition, the lack of waste LIB management implementation would interrupt the widespread deployment of EV markets owing to the potential risks of the supply chain of critical materials used in EVs.

As the electrification of the transportation sector intensifies, many countries have put their efforts into securing material supply chains for EVs. In 2021, the United States government proposed an investment of up to \$174 billion in EV programs focused on re-establishing primary metals refining and manufacturing, and creating new recycling capabilities. In particular, the key metal elements used in manufacturing Li-ion cathodes, such as Co, Li, and Ni, are exposed to various supply chain risks because of their geographic concentration. For example, 70% of Co was mined from the Democratic Republic of Congo in 2018, and 67% of refined Co metal is currently produced in China. The geographic concentration of these raw materials makes the supply chain vulnerable to disruptions and price volatility, which subsequently affects the growth of the EV sector. Recycling or reusing valuable cathode materials from EOL batteries could help lower the dependence on mining cathode raw materials, addressing supply risks and the rise in commodity prices.

Direct LIB recycling—introduced first in the early 2000s¹³—has gained significant attention from the academic and industrial sectors because of its environmental and economic benefits compared to other recycling technologies. This recycling approach focuses on the recovery and regeneration of cathode materials, which are the most valuable materials in LIBs. Direct cathode recycling is not required to break down the original functional structure of the cathode materials or dissolve them into solvents. Instead, it aims to regenerate spent cathode materials by addressing their Li deficiencies and structural defects. The cathode regeneration process is mainly based on the hypothesis that the EOL battery remaining at 80% of the original rated capacity contains a reusable form of the cathode with minor defects. To date, several

direct cathode recycling methods, including cathode healingTM,¹³ Etoile-Rebatt,¹⁴ electrochemical,¹⁵⁻¹⁸ solid-state sintering,¹⁹⁻²¹ hydrothermal,^{13, 22-24} and eutectic molten salt reaction²⁵ processes, have been utilized to recover and regenerate spent cathode materials without decomposition into substituent elements, as compared with classical hydrometallurgy,²⁶ pyrometallurgy,²⁷ and biometallurgy²⁸ processes, which often use concentrated acids and generate large amounts of waste solutions.

Although previous studies have successfully demonstrated the feasibility of regenerating spent cathode materials, they have mainly focused on the development of cathode regeneration processes. There remains a lack of fundamental studies on how the cathode regeneration process addresses several degradation factors, such as morphological, structural, and chemical defects, existing in the spent cathode. Most previous studies utilized aged EOL batteries with an unknown state of health (SOH)^{14, 19-21, 24} or inhouse EOL batteries artificially made under specific cycling conditions^{15-18, 22, 23, 25}. These types of EOL batteries make it difficult to systematically examine the regeneration process for several reasons: 1) the EOL cathode is degraded through multiple mechanisms that are strongly coupled with each other; 2) it is difficult to control the state of the EOL cathode; and 3) the complete removal of the binder and carbon additive from the EOL cathode during liberation/separation is challenging, which would impact the regeneration process. Therefore, this study employed chemically delithiated LiCoO₂ (LCO) cathodes that are analogous to EOL LCO cathodes but free of impurities, such as carbon black, binder, and surface layer, to fundamentally elucidate the effectiveness of cathode regeneration. LCO is relatively simple in terms of degradation and healing mechanisms compared to other cathode chemistries, which significantly helps precisely evaluate the effectiveness of cathode regeneration.

This study aimed to examine how direct cathode regeneration can repair and rejuvenate spent cathode materials at different levels of SOH, using chemically delithiated cathodes. Chemical delithiation, which has been extensively employed in conducting fundamental studies on cathode materials, enables the facile preparation of large quantities of cathodes at different degrees of delithiation and the precise control of the targeted Li stoichiometry in cathodes. Although it is still debatable how accurately the chemical delithiation process can represent electrochemical delithiation, it is generally accepted that chemically and electrochemically delithiated cathodes exhibits similar crystal structure features, electronic properties, thermal stability, and non-uniform Li distribution at the particle level.²⁹⁻³¹ In this study, chemically delithiated LCO, representing spent LCO, was systematically evaluated in terms of morphology, crystallinity, phase, and electrochemical performance to understand the state of LCO before regeneration (Section 3.1). Thereafter, we elucidated how LCOs at different degrees of delithiation are effectively regenerated by hydrothermal treatment with short annealing (Section 3.2).

2. Experimental

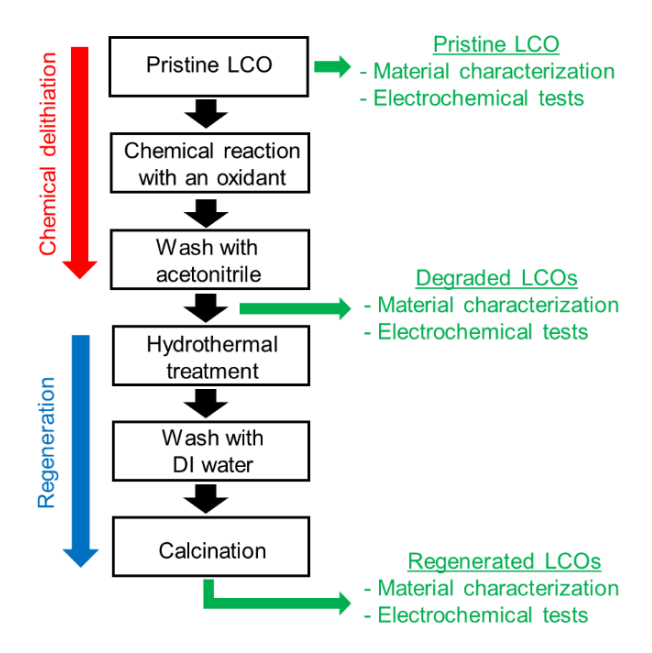


Fig. 1. Schematic flowchart of the experimental procedure.

Figure 1 shows a schematic of the overall experimental procedure of this study. This process involves two main steps: chemical delithiation and regeneration. To simulate cathode materials at different levels of degradation, pristine LCO (Sigma Aldrich) was chemically delithiated by stirring the LCO powder with the strong oxidizer NO₂BF₄ in an acetonitrile solution for two days under an argon atmosphere. During this step, a certain amount of Li in LCO was chemically extracted according to the following reaction:

$$LiCoO_2 + xNO_2BF_4 \rightarrow Li_{(1-x)}CoO_2 + xNO_2 + xLiBF_4$$
 (1)

Chemically delithiated LCO represents a Li-deficient, less-ordered LCO that is typically observed in spent LIBs. To produce LCOs with different levels of Li loss (i.e., Li_{0.8}CoO₂ and Li_{0.6}CoO₂), we mixed pristine LCO powder with the oxidant using different stoichiometric ratios. After chemical delithiation, the products formed were centrifuged and washed three times with acetonitrile to remove LiBF₄ or unreacted residue of NO₂BF₄. The final products were vacuum-dried overnight in a vacuum oven.

To regenerate the two model LCOs at different degrees of delithiation, the chemically delithiated LCO powders were loaded into a 50 ml Teflon-lined autoclave filled with 35 ml of 4 M lithium hydroxide (LiOH) solution. The autoclave was maintained in a furnace at 200°C for 20 h. The treated powders were thoroughly washed with deionized water and dried before calcination. Finally, the powders were calcinated at 800°C for 6 h under atmospheric conditions.

To evaluate the electrochemical performance of the pristine, delithiated, and regenerated LCOs, LCO powders were mixed with KS6L graphite (2 wt.%), Super C65 (3 wt. %), and polyvinylidene fluoride (PVDF) (5 wt.%, 7200 Kureha) dissolved in N-methyl-pyrrolidine (NMP). The resulting slurries were cast on an aluminum foil, followed by overnight vacuum drying at 100°C. The active material loading was approximately 10.5 mg/cm². 2032 coin-cells were assembled in an Ar-filled glove box with a half-cell configuration (Li foil/LCO). The electrolyte was a 1.2 M solution of LiPF₆ in ethylene carbonate (EC) and ethyl methyl carbonate (EMC) in a 1:1 volume ratio. Galvanostatic cycling was performed in the potential range of 3.0-4.2V at a C/5 rate using a battery tester. Electrochemical impedance spectroscopy (EIS) tests were performed in the fully discharged state (i.e., 3.0 V vs. Li/Li⁺) in the frequency range of 500 kHz to 0.1 Hz by applying a sinusoidal potential amplitude of 5 mV.

To characterize the LCO materials in terms of morphology, phase, crystallinity, and Li content, scanning electron microscopy (SEM, JEOL 7800f, Tokyo, Japan), X-ray diffraction (XRD, Bruker D8 Discover, USA), and thermogravimetric analysis (TGA, TA Instruments SDT-Q600, New Castle, DE, USA) were conducted, respectively. XRD was performed over a 2θ angle range of 10–70° at a scanning rate of 0.85°/min. TGA was performed at a ramping rate of 5°C/min over a temperature range of 25–800°C in argon flow (at a rate of 10L/min).

3. Results and Discussion

3.1 Material characteristics and electrochemical performance of delithiated LCO cathodes

In Section 3.1, we systematically analyze the structural, chemical, morphological, and electrochemical characteristics of chemically delithiated LCOs to (1) elucidate how degraded LCOs are regenerated through a direct recycling method and (2) investigate how chemically delithiated LCOs resemble aged LCOs from EOL batteries. The material characteristics and electrochemical performance of chemically delithiated LCOs are further compared with those of regenerated LCOs in Section 3.2.

Figure 2 shows the XRD patterns of pristine and delithiated LCO materials. Both Li-deficient LCOs (i.e., Li_{0.8}CoO₂ and Li_{0.6}CoO₂) retained their original layered structure with space group R-3m after chemical delithiation; however, the full width at half maximum (FWHM) of the XRD peaks broadened and their intensities decreased as the level of Li extraction in LCO increased. This indicates that the crystal structure of LCO is less ordered because Li is extracted from the lattice structure. Furthermore, the XRD patterns of delithiated LCOs did not exhibit any new peaks that were not found in pristine LCO, suggesting that undesirable impurities or phase transitions were absent in the chemically delithiated LCOs. The lower crystallinity of delithiated LCOs was further confirmed by the intensity ratio of I₀₀₃/I₁₀₄. The I₀₀₃/I₁₀₄

intensity ratio is a disorder indicator of the atomic positions of Li and Co cations in the LCO crystal structure.³² More importantly, this intensity ratio is closely related to the degree of cation mixing, which is detrimental to the electrochemical performance of the layered cathodes.^{33, 34} In the ordered LCO crystal structure, Li and Co ions occupy the 3b and 3a octahedral sites in a cubic, close-packed oxygen sub-lattice.³⁴ When Li/Co cation mixing occurs, some Co atoms migrate into part of the Li octahedral sites, leading to a disordered cation arrangement in the crystal structure. Thus, the lower intensity ratio of (003) to (104) is correlated with a higher degree of cation mixing, a deteriorated layered structure, and reduced cyclability.

Table 1 lists the I_{003}/I_{104} ratio of the deliahited LCOs at different degrees in comparison to the pristine LCO. The I_{003}/I_{104} ratio of LCO decreased substantially after chemical delithiation, indicating the disordering of the LCO crystal structure caused by Li/Co cation mixing. With increasing delithiation of LCO, the I_{003}/I_{104} ratio decreased further, which is consistent with results of a previous study.³² This signifies that the higher degrees of disordering and cation mixing of the layered LCO were more pronounced with higher Li removal.

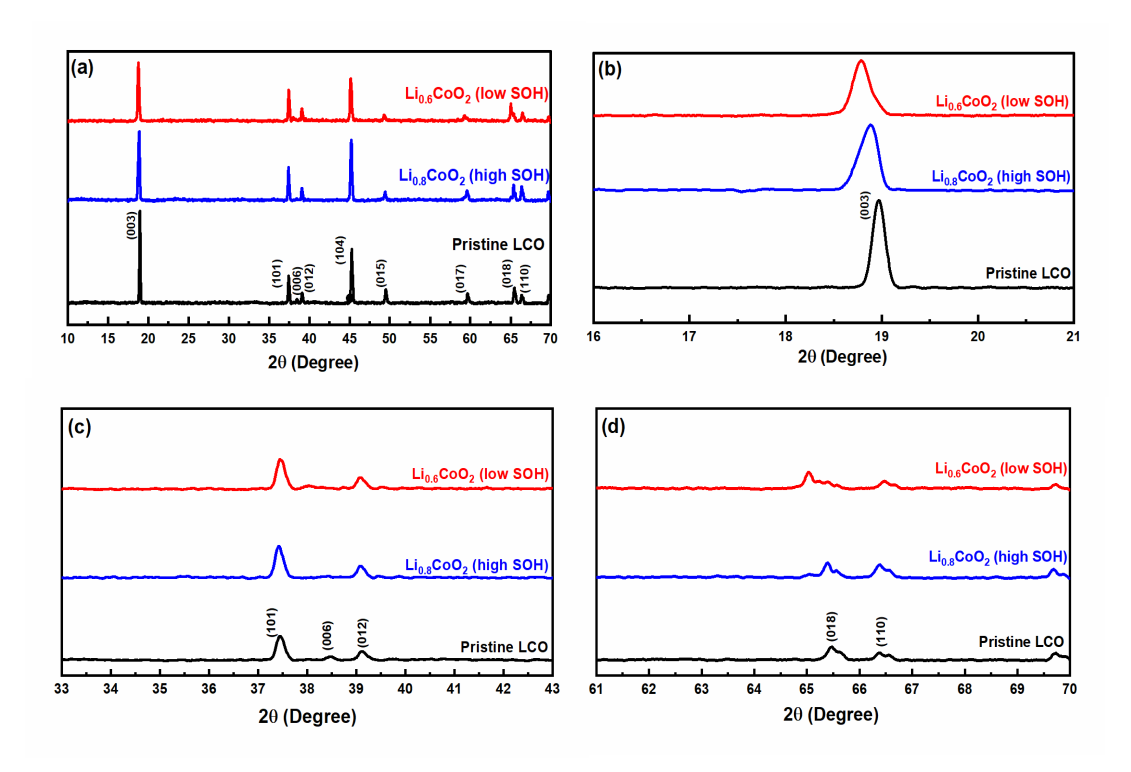


Fig. 2. XRD patterns of pristine and chemically delithiated LCOs (a), and their enlarged views (b-d).

Table 1. The intensity ratio of I_{003}/I_{104} for pristine and delithiated LCO materials.

Sample	$I_{(003)}/I_{(104)}$
Pristine LCO	2.99
Chemically delithiated LCO, 20% Li extraction	2.21
Chemically delithiated LCO, 40% Li extraction	1.90

The Li deficiency in chemically delithiated LCOs was evaluated by comparing the (003) diffraction peaks of the pristine and delithiated LCOs. As shown in Figure 2b, the (003) peak shifted to the left, while its intensity decreased with broadening. This indicates that the synthesized LCOs were at different degrees of delithiation, and their c-lattice parameters increased compared to those of the pristine LCO.³⁰ The lower the (003) diffraction angle, the higher the delithiated LCO. Upon Li extraction from the LCO lattice structure, the a-lattice parameter and the intensity ratio of I₀₀₃/I₁₀₄ are known to decrease, whereas the c-lattice parameter increases.^{30, 31} Other XRD peaks also indicate a change in the LCO lattice structure, as a certain amount of Li was extracted from the structure. As shown in Figure 2c and d, the (006) diffraction peak disappeared, and the peak split of (018)/(110) became wider for chemically delithiated LCOs than for pristine LCO. LCO delithiated at a higher degree (i.e., Li_{0.8}CoO₂) showed a wider peak split of (018)/(110) than LCO delithiated at a lower degree (i.e., Li_{0.8}CoO₂), indicating that the disordering of the LCO crystal structure was more pronounced with higher delithiation.

XRD analysis confirmed that the chemically delithiated LCO samples targeted for Li_{0.8}CoO₂ and Li_{0.6}CoO₂ had a Li-deficient, disordered layer structure compared to the original LCO crystal structure. In terms of Li deficiency and crystal structure disordering, chemically delithiated LCOs are somewhat similar to spent LCOs from EOL batteries.^{16, 20, 23, 32} According to a previous study, Li_{0.8}CoO₂ and Li_{0.6}CoO₂ samples reasonably represent the spent LCOs collected from EOL batteries at high and low SOH, respectively.³² Although there is a discrepancy in the literature regarding the existence of the Co₃O₄ phase for spent LCO,^{16, 20, 23, 32} spent LCO retains the original layer structure; however, the structure is expected to be disordered with Li loss. The Co₃O₄ phase presence of the spent LCO may depend on the battery cycling conditions and how the LCO active material is separated from the battery. The major difference between chemically delithiated and spent LCO materials is the presence of surface layers on the material. However, the absence of such surface layers on the chemically delithiated LCO would be beneficial in accurately evaluating how the recovery of Li deficiency and the crystal structure of the delithiated LCOs contribute to improving the electrochemical performance after regeneration. In Section 3.2, we reveal how a Li-deficient, disordered layer structure of LCOs returns to the original layered structure with full Li stoichiometry after the regeneration process.

The Li deficiency in the chemically delithiated LCO samples was further observed using TGA. Figure 3 shows that the thermal stability of delithiated LCOs is much lower than that of pristine LCO. While pristine LCO (i.e., LiCoO₂) showed no weight loss up to 800°C, chemically delithiated Li_{0.8}CoO₂ and Li_{0.6}CoO₂ exhibited total weight losses of 1.31% and 3.53%, respectively. It is clear that increasing the Li loss from the layered LCO crystal structure resulted in a lower decomposition onset temperature and higher amount of weight loss. The observed weight losses for the delithiated LCOs were in good agreement with

the total amounts of liberated oxygen from Li_{0.81}CoO₂ and Li_{0.65}CoO₂, respectively.³⁵ This suggests that the weight losses of the chemically delithiated LCOs are related to oxygen release from the layered structure, and the LCO with a higher degree of Li loss (i.e., Li_{0.6}CoO₂) is more unstable, owing to the release of more oxygen from the layered structure at elevated temperatures.³⁵ Furthermore, the results confirmed that chemical compositions of the delithiated LCO samples were close to the target compositions of Li_{0.8}CoO₂ and Li_{0.6}CoO₂.

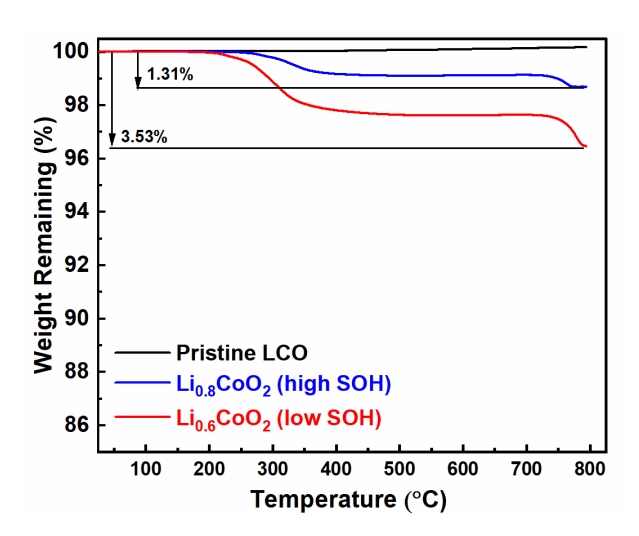


Fig. 3. TGA curves of pristine, chemically delithiated LCO materials.

For chemically delithiated LCOs, two stages of weight loss were observed in the ranges of 320°C to 350°C and 750°C to 800°C. According to previous studies,³⁵⁻³⁷ the former is attributed to oxygen loss caused by the partial decomposition of delithiated LCO to Co₃O₄, whereas the latter corresponds to additional oxygen loss resulting from decomposition reactions from Co₃O₄ to CoO followed by CoO to Co. It should be noted that these decomposition reactions can be accelerated in the presence of residual electrolyte, polymeric binder, and carbon additive.³⁷ Thus, spent LCOs containing a small amount of residual electrolyte, binder, or carbon additive would display a higher weight loss than chemically delithiated LCOs.

The TGA results suggest that the spent LCOs retrieved from EOL batteries at low and high SOHs are structurally and thermally unstable because of the Li loss from the layered structure. The spent LCO at a low SOH would exhibit lower thermal stability than LCO at a high SOH. In Section 3.2, we explore how the thermal instability of LCOs at different degrees of SOH is recovered after LCO regeneration.

The surface morphology of the chemically delithiated LCO samples was also investigated using SEM. The SEM analysis revealed that chemical delithiation resulted in changes in the LCO morphology to

some extent. Consistent with previous studies, a few pitting patterns and microcracks were observed for the chemically delithiated LCOs, as shown in Figure 4.^{29, 38, 39} These morphological changes could be induced by localized stress resulting from rapid Li extraction from the layered structure in the presence of a high concentration of the strong oxidant, NO₂BF₄.²⁹ The microcracks observed in chemically delithiated LCO may resemble those observed in spent LCO to some extent. It is commonly known that microcracking and fracturing of LCO occur after long-term cycling.⁴⁰ In Section 3.2, we investigate whether the modified morphology of LCO can be overcome after regeneration and how morphological changes affect the electrochemical performance of the regenerated LCO.

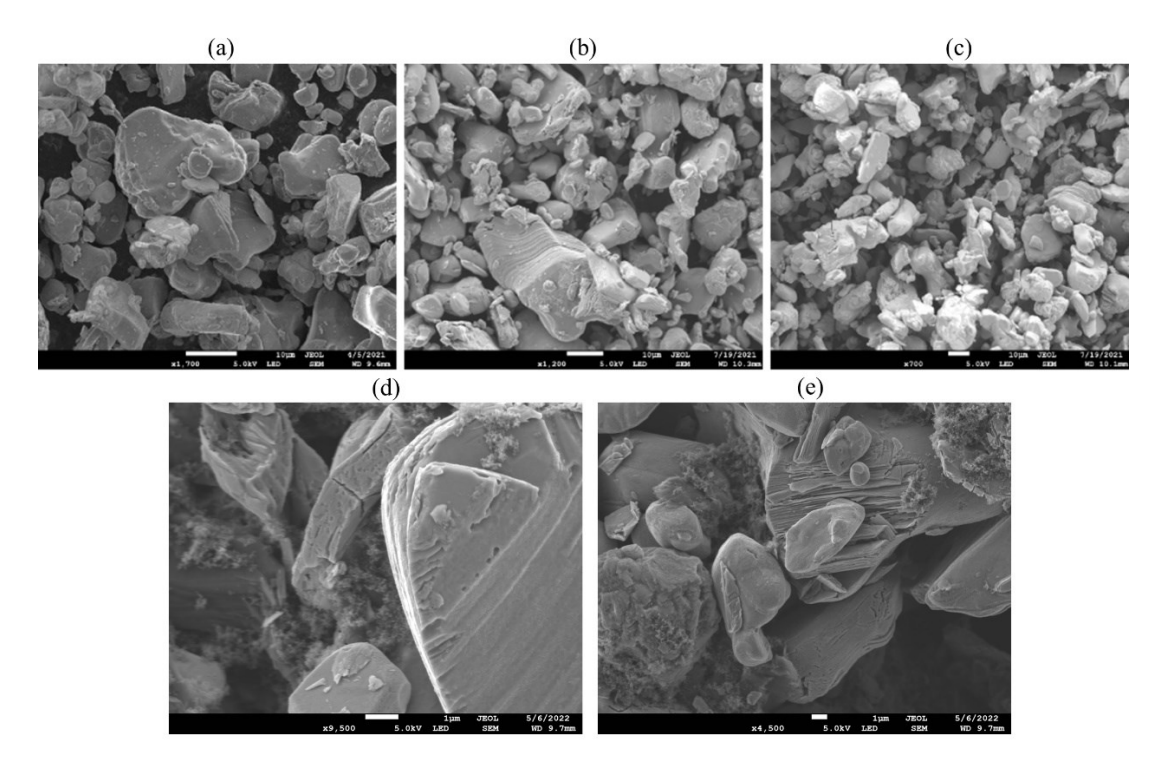


Fig. 4. SEM images of (a) pristine, (b) chemically delithiated Li_{0.8}CoO₂, and (c) chemically delithiated Li_{0.6}CoO₂. SEM images (c, d) of chemically delithiated Li_{0.6}CoO₂ that show a few pitting and microcrack patterns.

In addition to the material properties, the electrochemical characteristics of the chemically delithiated LCOs were systematically evaluated before direct cathode regeneration. Figure 5a and b show the charge-discharge profiles of pristine and chemically delithiated LCOs at the first and third cycles, respectively. The first discharge capacity of Li_{0.8}CoO₂ and Li_{0.6}CoO₂ was 112.7 mAh and 84.9 mAh/g, close to 80% and 60% of the discharge capacity of the pristine LCO, respectively. The reduced capacities further confirmed the Li deficiency in chemically delithiated LCOs, and that the delithiated LCOs were close to the chemical compositions of Li_{0.8}CoO₂ and Li_{0.6}CoO₂. Interestingly, the CV charge capacity of delithiated

LCOs, an indicator of cell resistance, was significantly high at the first cycle; this was not observed in the corresponding pristine LCO. This could be associated with the disruption of the ordered LCO lattice structure resulting from the Li loss. The high CV charge capacity of the chemically delithiated LCOs decreased considerably after the first cycle, as shown in Figure 5b. This indicates that when Li ions, being removed from the delithiated cathode structure during charging, electrochemically insert into the structure during discharging, the LCO structure is re-established to some extent. Based on the slight increase in discharge capacity of Li_{0.8}CoO₂ and Li_{0.6}CoO₂ after a few cycles (121.2 mAh/g and 98.5 mAh/g at the third cycle, respectively, Fig. 5b), the lattice structure of delithiated LCOs had potential for being re-established while it was electrochemically relithiated. Obviously, the Li metal in the half-cells provided additional Li ions to some extent during cycling. However, the structure of delithiated LCOs cannot be fully recovered and relithiated electrochemically; therefore, chemically delithiated LCOs still exhibited a higher CV charge capacity during the third cycle, indicating higher cell resistance than pristine LCO. The high cell resistance of chemically delithiated LCOs is analogous to that of spent LCOs in EOL cells.

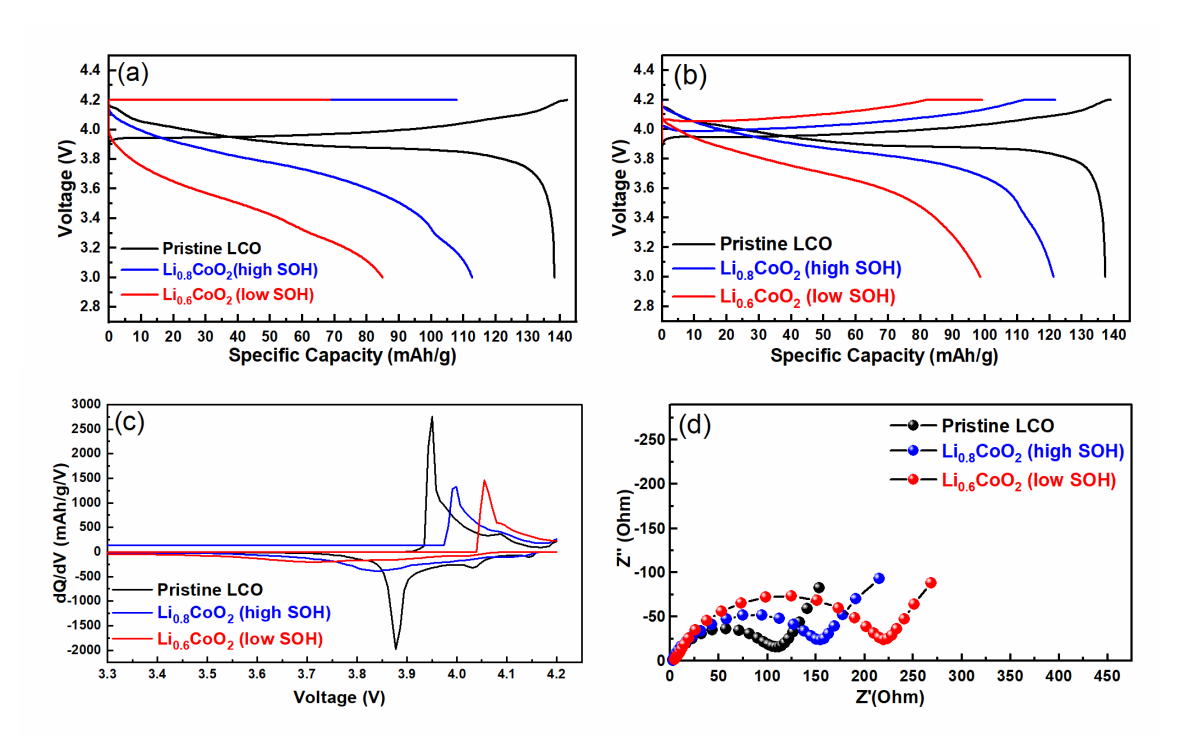


Fig. 5. Comparisons of (a) first cycle and (b) third cycle charge-discharge profiles, (c) third cycle differential capacity (dQ/dV) plots, and (d) Nyquist plots of pristine LCO, chemically delithiated Li_{0.8}CoO₂, and Li_{0.6}CoO₂. Cells were cycled at a C/5 rate. EIS tests were performed at the fully discharged state after 3 cycles.

Owing to the high cell resistance of chemically delithiated LCOs, they displayed larger cell polarization than pristine LCO, as clearly observed in their voltage plateau and dQ/dV characteristics. As shown in Figure 5b, the charge voltage plateaus of Li_{0.8}CoO₂ and Li_{0.6}CoO₂ were approximately 4.0 and

4.05 V, respectively, which were higher than the voltage plateau 3.95 V of pristine LCO. Li_{0.6}CoO₂ showed larger cell polarization than Li_{0.8}CoO₂. The dQ/dV curves also showed that the oxidation and reduction peaks of Li_{0.6}CoO₂ shifted to a higher potential for charge and a lower potential for discharge, respectively, compared with those of Li_{0.8}CoO₂ and pristine LCO. The reduction in the peak intensities for chemically delithiated LCOs occurred due to their reduced capacity resulting from Li loss after chemical delithiation.

To further understand the high cell resistance of the chemically delithiated LCOs, impedance spectra were obtained by EIS (Fig. 5d). A clear distinction between the pristine and delithiated LCO samples was observed in the dimensions of the semicircle in the medium-frequency range, which mainly corresponds to the charge transfer resistance. ⁴¹ The charge transfer resistance increased with an increase in the extent of delithiation in LCO. Because the charge transfer resistance is strongly dependent on the level of Li intercalation in the electrode, the increase in the charge transfer resistance of chemically delithiated LCOs can be associated with Li loss in the crystal structure of delithiated LCO. ⁴² It should be noted that Li loss deteriorated the ratio of disordering in the crystal LCO structure (Table 1), which can be the main reason for the increase in the charge transfer resistance of delithiated LCO. ^{18, 43} This indicates that more energy is required to complete the charge transfer reaction when Li intercalates into a partially disordered structure, with respect to the fully ordered LCO crystal structure. Additionally, the changes in the surface morphology of delithiated LCOs could contribute to the increase in the charge transfer resistance. Because the corrosion of active electrode materials is closely coupled with charge transfer reactions at the electrode/electrolyte interfaces, the pitting and microcrack patterns observed in chemically delithiated LCOs (Fig. 4) could be another contributor to the increased charge transfer resistance. ⁴⁴

In contrast, the intersections on the real axis at high frequencies and the linear portion at low frequencies (i.e., Warburg impedance) were nearly identical for both pristine and chemically delithiated LCOs. The high-frequency resistance at which the impedance spectrum intercepts the real axis represents the ohmic resistance of the cell, which originates from the electronic resistance of electronic and ionic conductive materials, such as connectors, contacts, electrodes, and electrolytes. The low-frequency slope of the Warburg tail of the impedance spectrum is ascribed to solid-state diffusion in the cathode host structure. The low-frequency slopes for the LCO samples were close to 45°, which suggests that chemical delithiation did not cause any severe LCO lattice distortion that could interrupt Li diffusion in the host structure.

Figure 6 shows the rate capability and cycle performance of chemically delithiated Li_{0.8}CoO₂ and Li_{0.6}CoO₂, compared with those of pristine LCO. As expected, chemically delithiated LCOs showed inferior rate capability and cycle performance compared to pristine LCO, which resembles the electrochemical performance of end-of-life LCO cathodes. The delithiated Li_{0.6}CoO₂, representing LCO at low SOH,

showed a poorer rate and cycle performance than the delithiated Li_{0.8}CoO₂, which represents LCO at high SOH. For instance, capacity retention of 61.03% was observed for delithiated Li_{0.6}CoO₂ after 100 cycles, with respect to the rated initial capacity after the formation cycle, which was much lower than the capacity retention of 81.78% observed for delithiated Li_{0.8}CoO₂. In addition, it was found that the rate performance of delithiated Li_{0.6}CoO₂ significantly deteriorated at high C rates (1C and 2C).

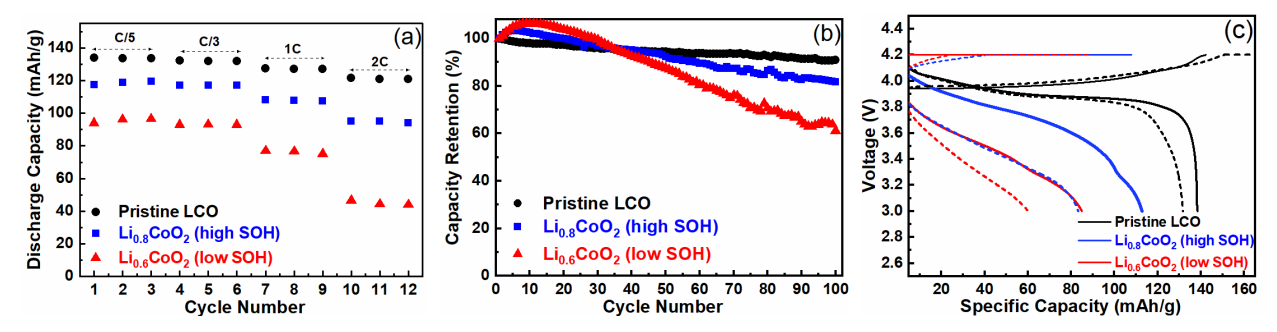


Fig. 6. Comparisons of (a) rate performance, (b) cycling performance, and (c) charge-discharge curves (solid lines: after 3 cycles; dotted lines: after 100 cycles) of pristine LCO, chemically delithiated Li_{0.8}CoO₂, and Li_{0.6}CoO₂. The cells were cycled in the voltage range of 3.0 to 4.2 V at a C/3 rate.

In summary, we systematically evaluated the material and electrochemical characteristics of two different chemically delithiated LCOs and compared them with those of pristine LCO. Based on this information, we confirmed that chemically delithiated Li_{0.6}CoO₂ and Li_{0.8}CoO₂ resemble the spent LCOs at different degrees of SOH. Furthermore, it clearly revealed the states of delithiated LCOs before regeneration, which is a prerequisite for evaluating their improvements after regeneration. In Section 3.2, we elucidate the mechanisms of direct cathode regeneration by comparing the material and electrochemical characteristics of the delithiated and regenerated LCOs and investigating whether the model LCOs at different degrees of delithiation can be recovered to a level similar to that of pristine LCO.

3.2 Material characteristics and electrochemical performance of regenerated LCO cathodes

To provide fundamental insights into direct cathode regeneration, we examined how the material properties and electrochemical performance of delithiated LCOs change after cathode regeneration. To evaluate whether the regenerated LCOs are comparable to pristine LCO, we also compared the material properties and electrochemical performance with those of pristine LCO.

Figure 7 shows XRD patterns of pristine, delithiated, and regenerated LCOs and their TGA profiles. As shown in Fig. 7a, the crystallinity of both Li_{0.6}CoO₂ and Li_{0.8}CoO₂ was significantly improved after regeneration. The phase of the regenerated LCOs was similar to that of the pristine LCO. No additional phase was observed for the regenerated LCOs. The result suggests that spent LCOs at different levels of SOH can be re-established to form their original crystal structures. This can be further confirmed by the

changes in (003) and (006) diffraction peaks after regeneration. For both Li_{0.6}CoO₂ and Li_{0.8}CoO₂, the (003) peak shifted back to its original angle, while its peak intensity increased significantly after regeneration (Fig. 7b and c). This indicates the insertion of Li ions into the LCO crystal structure, thereby recovering the original layered structure. The change in (006) diffraction peak further proved that the disordered crystal structures of Li_{0.6}CoO₂ and Li_{0.8}CoO₂ were recovered to a level similar to that of their original layered structure. The (006) peak that disappeared from both Li_{0.6}CoO₂ and Li_{0.8}CoO₂ became more visible and sharper after regeneration (Fig. 7d and e). This also implies that the hydrothermal-based regeneration process facilitated filling up the Li deficiency in the delithiated LCOs, thereby improving the crystallinity of the layered structure.

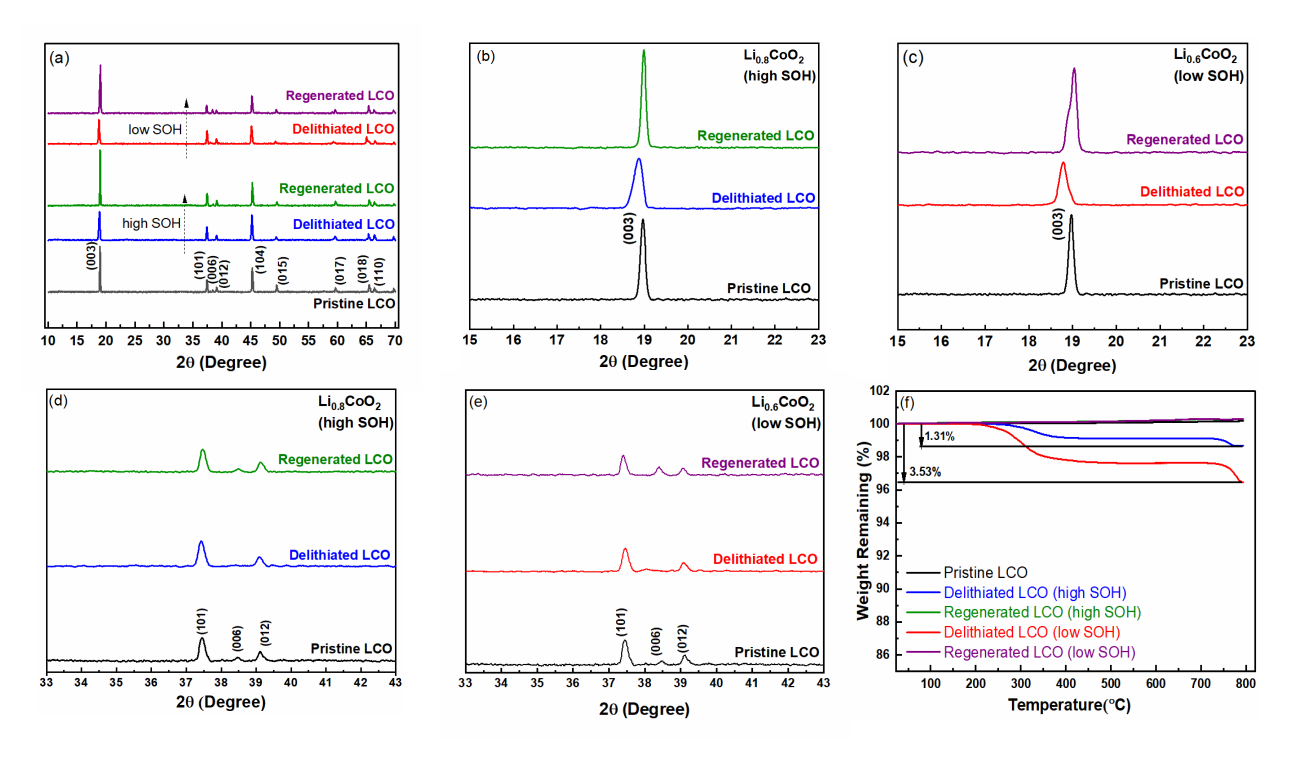


Fig. 7. Comparisons of XRD patterns (a,b,c,d,f) and TGA profiles (f) of pristine, delithiated, regenerated LCOs. Enlarged views of (003) diffraction (b,c) and (101)/(006)/(012) diffraction (d,e) peaks for pristine, delithiated, regenerated LCOs.

TGA analysis also confirmed that the crystal structures of Li_{0.6}CoO₂ and Li_{0.8}CoO₂ were reestablished after regeneration. As shown in Figure 7f, the regenerated LCOs exhibited thermal stability comparable to that of pristine LCO. No weight loss was observed in the TG curves of the LCOs regenerated from Li_{0.6}CoO₂ and Li_{0.8}CoO₂, which is clear evidence of the restoration of oxygen and lithium deficiencies in the LCO lattice structure. If the regenerated LCOs were still delithiated states with Li deficiency, there would have been a certain amount of weight loss at elevated temperatures, as observed in the delithiated LCO samples. The slight increases in weights of the regenerated LCOs possibly occurred due to buoyancy

effects caused by the decrease in the density of the surrounding gas upon heating. This buoyancy effect was also noticeable in the pristine LCO sample, which resulted in slight weight gain.

Our results suggest that the deteriorated crystal structure and Li deficiency in spent LCOs at different levels of SOH can be recovered after the hydrothermal-based regeneration process. Thereafter, we further investigated whether the restoration of the material characteristics of LCO eventually led to regaining the electrochemical performance comparable to that of pristine LCO.

Figure 8 compares the electrochemical performance and impedance spectra of delithiated and regenerated LCOs. The corresponding electrochemical data for pristine LCO are also presented for reference (Fig. 8a, b, and c). Both LCOs regenerated from chemically delithiated Li_{0.8}CoO₂ and Li_{0.6}CoO₂ restored their original capacities, thereby showing a similar discharge capacity (approximately 140.5 mAh/g) to that of pristine LCO. It was also noticeable that the CV charge duration at the first cycle was significantly reduced after regeneration (Fig. 8d). Furthermore, the voltage plateau at which (de)intercalation reactions occur (approximately 3.9 V) is well defined for regenerated LCOs, similar to pristine LCO. These results indicate that the Li loss in delithiated LCOs was reinstated during regeneration, re-establishing the lattice structure. Consequently, the delithiated LCOs regained their electrochemical performances. Notably, however, the CV capacity observed in the regenerated LCOs was slightly higher than that of the pristine LCO, although it was significantly lower than that of the delithiated LCOs. Therefore, the regenerated LCOs may not be completely repaired to attain a sufficiently low cell resistance, comparable to that of pristine LCO.

To further explore the characteristics of the cell resistance of the regenerated LCOs, the impedance spectra of pristine (Fig. 8c), delithiated and regenerated LCOs (Fig. 8f) were compared. The charge transfer resistance of LCO regenerated from Li_{0.6}CoO₂ (low SOH) was larger than that of LCO regenerated from Li_{0.8}CoO₂ (high SOH). More interestingly, while the charge transfer resistance of Li_{0.6}CoO₂ (high SOH) was reduced after regeneration, the charge transfer resistance of Li_{0.6}CoO₂ (low SOH) remained almost constant, without any improvement. This may suggest that the LCO at high SOH, which is relatively less damaged at both the particle and lattice levels, can restore its structural functionality and cell resistance. Alternatively, the difference between changes in the impedance spectra of Li_{0.6}CoO₂ and Li_{0.6}CoO₂ after regeneration can be attributed to the deep chemical delithiation of Li_{0.6}CoO₂, which could induce non-recoverable microcracks/pits on the particle surface and severe lattice disordering.³⁹ There may be differences in the structural and morphological features between the chemically delithiated and electrochemically delithiated samples. While spent LCOs that undergo electrochemical cycling are likely to present cracked particles to some extent, chemically delithiated LCOs can exhibit highly localized morphological defects, such as pitting, along with a higher specific surface area.³⁹ Nevertheless, the EIS

results suggest that end-of-life LCOs involving severe morphological and structural changes after extensive cycling may not recover their original functionality after regeneration.

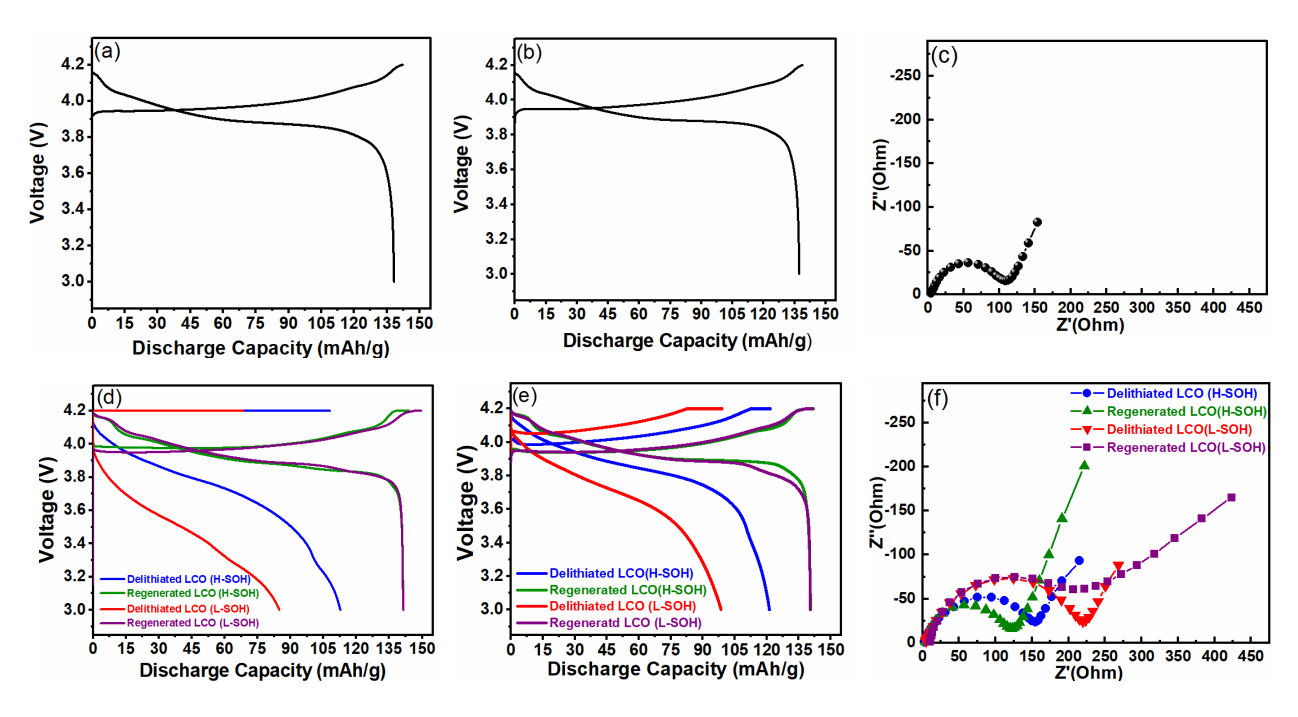


Fig. 8. First cycle (a) and third cycle (b) charge-discharge curves, and Nyquist plot (c) of the reference, pristine LCO (black). Comparison between first cycle (d) and third cycle (e) charge-discharge curves, and Nyquist plots (f) of delithiated [Li_{0.8}CoO₂: H-SOH (blue), Li_{0.6}CoO₂: L-SOH (red)] and regenerated [H-SOH (green), L-SOH (purple)] LCOs. EIS was performed at the fully discharged state after 3 cycles.

Based on the EIS results, it was speculated that the rate capability of the regenerated LCO from $Li_{0.6}CoO_2$ may not be comparable to that of pristine LCO, although the reversible capacity of $Li_{0.6}CoO_2$ was significantly enhanced after regeneration. This argument was further supported by the rate test results presented below.

Figure 9a and b compare the rate capabilities of the pristine, delithiated and regenerated LCOs. Overall, the rate capabilities of both Li_{0.8}CoO₂ and Li_{0.6}CoO₂ significantly improved after regeneration. More interestingly, the rate capability of the regenerated LCOs displayed similar performance at C/5, C/3, and 1C rates compared to pristine LCO. Nevertheless, at a higher C-rate (2C), the regenerated LCOs displayed a lower capacity utilization than pristine LCO. These results suggest that the rate performance of spent LCOs at different levels of SOH can be regained after regeneration. However, it may be challenging to regenerate the spent LCO to the point where it retrieves its original high-rate performance.

Simultaneously, the results indicated that the cell resistance observed for the regenerated LCOs was not high enough to affect the electrochemical kinetics at low and moderate C-rates. The cell resistance of the regenerated LCOs only affected the electrochemical performance at a high current density (2C).

Thus, the cycle stabilities of both Li_{0.8}CoO₂ and Li_{0.6}CoO₂ at the C/3 rate were notably improved after regeneration, as shown in Fig. 9d. The regenerated LCOs showed cycle performance comparable to that of the pristine LCO (Fig. 9c). However, it should be noted that the cycle performance at a high C-rate may not be comparable to that of pristine LCO, especially for the regenerated LCO from Li_{0.6}CoO₂, which had a relatively higher cell impedance than the others. Most previous studies have not systematically investigated the cell resistance of regenerated cathode materials in comparison to the corresponding pristine materials, while focusing on the recovery of the reversible capacity and cycle stability after direct cathode regeneration. ^{13, 15, 19, 21, 23} Our study suggests that the effectiveness of direct cathode regeneration should be further evaluated in terms of the rate capability and high-rate performance.

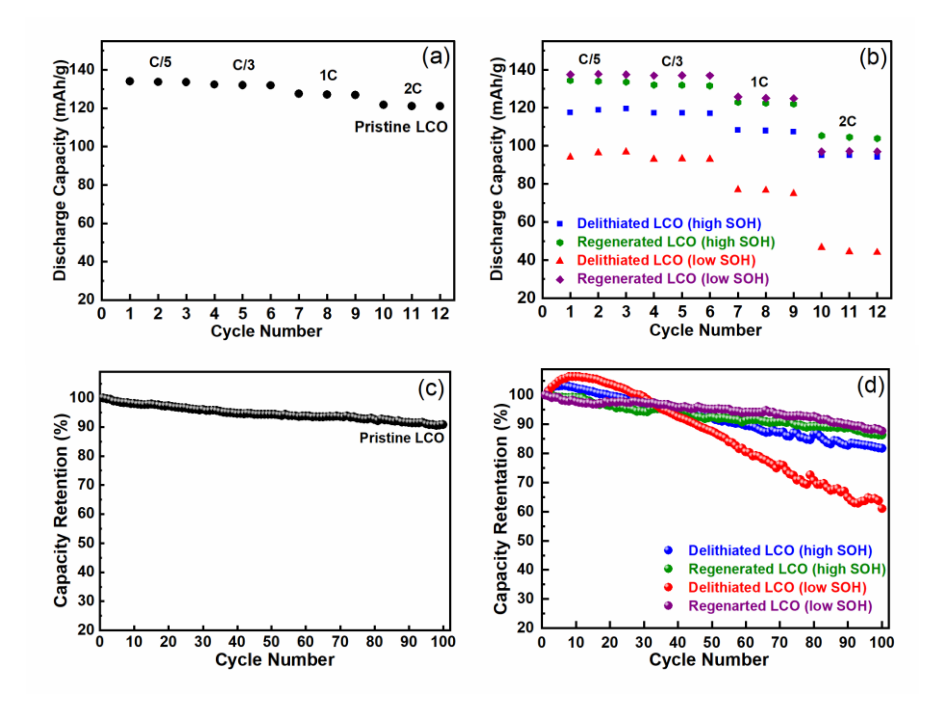


Fig. 9. Comparisons of rate capability (a, b) and cycle performance (c,d) of the pristine, delithiated and regenerated LCOs. Long-term cycle tests was performed at a C/3 rate.

4. Conclusions

This study fundamentally investigated how spent LCOs at different levels of SOH were regenerated to regain their original material and electrochemical characteristics using chemically delithiated LCO materials. The chemical delithiation approach enabled us to produce two different delithiated LCOs, which were analogous to spent LCOs at different levels of SOH, by controlling the Li content in LCO. The delithiated LCOs were free of carbon black, PvdF binder, and surface layer, which provided a better opportunity to precisely evaluate the effectiveness of direct cathode regeneration. We elucidated how Li loss from the LCO lattice structure results in changes in LCO material characteristics, such as crystallinity,

lattice disordering, thermal stability, and morphology, and how these changes are related to the electrochemical performance. The delithiated LCOs (Li_{0.8}CoO₂ and Li_{0.6}CoO₂) exhibited lower capacity, inferior cycle stability, larger CV capacity, cell impedance, and polarization than pristine LCO, which resembled the characteristics of spent LCO.

The direct cathode regeneration process employed in this study was effective in rejuvenating the LCOs at different levels of SOH. The hydrothermal-based regeneration process re-established the lattice structure of delithiated LCOs (Li_{0.8}CoO₂ and Li_{0.6}CoO₂) while restoring the Li deficiency in the crystal structure. Consequently, significant improvements were observed after LCO regeneration in terms of crystallinity, lattice disordering, thermal stability, reversible capacity, cycle stability, and rate performance at low and moderate C-rates. The reversible capacity and cycle stability of the regenerated LCOs at a C/3 rate were comparable to those of the pristine LCO. However, the cell resistance of the regenerated LCOs was slightly higher than that of pristine LCO. In particular, the LCO at a higher level of SOH (Li_{0.6}CoO₂) was not fully regenerated and exhibited a similar level of cell resistance to that of pristine LCO. This led to a lower capacity utilization at a high C-rate (2C). It was speculated that morphological changes (e.g., microcracks) that may contribute to cell resistance were difficult to return to defect-free morphological conditions, even after completion of the regeneration process. Further studies are needed to verify whether direct cathode regeneration can resolve morphological changes, such as particle cracking, in spent cathode materials.

Our study provides valuable insights into the effectiveness of direct regeneration of spent cathodes at different levels of SOH. The spent cathode material can be repaired to resolve the issues associated with Li deficiency and lattice disorder of the material, thereby significantly improving its electrochemical performance. However, it may be challenging to fully recover the high-rate performance of spent cathodes using simple hydrothermal-based regeneration processes.

Acknowledgment

The authors gratefully acknowledge the Research Support Funds Grant (RSFG) provided by Indiana University-Purdue University Indianapolis (IUPUI). This work is also supported by the National Science Foundation under Grant No. 2138553.

References

- 1. Y. Gogotsi and P. Simon, *Science*, **334**, 917 (2011).
- 2. J. Rogelj, M. den Elzen, N. Höhne, T. Fransen, H. Fekete, H. Winkler, R. Schaeffer, F. Sha, K. Riahi and M. Meinshausen, *Nature*, **534**, 631 (2016).
- 3. A. Pehlken, S. Albach and T. Vogt, *The International Journal of Life Cycle Assessment*, **22**, 40 (2017).
- 4. D. L. Thompson, J. M. Hartley, S. M. Lambert, M. Shiref, G. D. J. Harper, E. Kendrick, P. Anderson, K. S. Ryder, L. Gaines and A. P. Abbott, *Green Chemistry*, **22**, 7585 (2020).
- 5. S. Wang and J. Yu, Waste Management & Research, 39, 818 (2021).
- 6. C. K. Lee and K.-I. Rhee, *Journal of Power Sources*, **109**, 17 (2002).
- 7. X. Zeng, J. Li and N. Singh, *Critical Reviews in Environmental Science and Technology*, **44**, 1129 (2014).
- 8. H. Aral and A. Vecchio-Sadus, *Ecotoxicology and Environmental Safety*, **70**, 349 (2008).
- 9. H. E. Melin, M. A. Rajaeifar, A. Y. Ku, A. Kendall, G. Harper and O. Heidrich, *Science*, **373**, 384 (2021).
- 10. A. Zeng, W. Chen, K. D. Rasmussen, X. Zhu, M. Lundhaug, D. B. Müller, J. Tan, J. K. Keiding, L. Liu, T. Dai, A. Wang and G. Liu, *Nature Communications*, **13**, 1341 (2022).
- 11. Q. Dehaine, L. T. Tijsseling, H. J. Glass, T. Törmänen and A. R. Butcher, *Minerals Engineering*, **160**, 106656 (2021).
- 12. A. Mayyas, D. Steward and M. Mann, *Sustainable Materials and Technologies*, **19**, e00087 (2019).
- 13. S. Sloop, L. Crandon, M. Allen, K. Koetje, L. Reed, L. Gaines, W. Sirisaksoontorn and M. Lerner, *Sustainable Materials and Technologies*, **25**, e00152 (2020).
- 14. D.-i. Ra and K.-S. Han, *Journal of Power Sources*, **163**, 284 (2006).
- 15. M. J. Ganter, B. J. Landi, C. W. Babbitt, A. Anctil and G. Gaustad, *Journal of Power Sources*, **256**, 274 (2014).
- 16. T. Yang, Y. Lu, L. Li, D. Ge, H. Yang, W. Leng, H. Zhou, X. Han, N. Schmidt, M. Ellis and Z. Li, *Advanced Sustainable Systems*, **4**, 1900088 (2020).
- 17. L. Zhang, Z. Xu and Z. He, ACS Sustainable Chemistry & Engineering, 8, 11596 (2020).
- 18. K. Lahtinen, E.-L. Rautama, H. Jiang, S. Räsänen and T. Kallio, *ChemSusChem*, 14, 2434 (2021).
- 19. J. Chen, Q. Li, J. Song, D. Song, L. Zhang and X. Shi, *Green Chemistry*, **18**, 2500 (2016).
- 20. S. Chen, T. He, Y. Lu, Y. Su, J. Tian, N. Li, G. Chen, L. Bao and F. Wu, *Journal of Energy Storage*, **8**, 262 (2016).
- 21. X. Song, T. Hu, C. Liang, H. L. Long, L. Zhou, W. Song, L. You, Z. S. Wu and J. W. Liu, *RSC Advances*, **7**, 4783 (2017).
- 22. Y. Shi, G. Chen, F. Liu, X. Yue and Z. Chen, *ACS Energy Letters*, **3**, 1683 (2018).
- 23. Y. Shi, G. Chen and Z. Chen, *Green Chemistry*, **20**, 851 (2018).
- 24. Q. Jing, J. Zhang, Y. Liu, W. Zhang, Y. Chen and C. Wang, *ACS Sustainable Chemistry & Engineering*, **8**, 17622 (2020).
- 25. Y. Shi, M. Zhang, Y. S. Meng and Z. Chen, Advanced Energy Materials, 9, 1900454 (2019).
- 26. W.-S. Chen and H.-J. Ho, *Metals*, **8**, 321 (2018).
- 27. A. Holzer, S. Windisch-Kern, C. Ponak and H. Raupenstrauch, *Metals*, **11**, 149 (2021).
- 28. B. Wang, X.-Y. Lin, Y. Tang, Q. Wang, M. K. H. Leung and X.-Y. Lu, *Journal of Power Sources*, **436**, 226828 (2019).
- 29. C. Tian, Y. Xu, D. Nordlund, F. Lin, J. Liu, Z. Sun, Y. Liu and M. Doeff, *Joule*, 2, 464 (2018).
- 30. S. Li, K. Li, J. Zheng, Q. Zhang, B. Wei and X. Lu, *The Journal of Physical Chemistry Letters*, **10**, 7537 (2019).
- 31. Y. Takahashi, N. Kijima, K. Dokko, M. Nishizawa, I. Uchida and J. Akimoto, *Journal of Solid State Chemistry*, **180**, 313 (2007).

- 32. L. E. Sita, S. P. da Silva, P. R. C. da Silva and J. Scarminio, *Materials Chemistry and Physics*, **194**, 97 (2017).
- 33. H. J. Kim, Y. Park, Y. Kwon, J. Shin, Y.-H. Kim, H.-S. Ahn, R. Yazami and J. W. Choi, *Energy & Environmental Science*, **13**, 286 (2020).
- 34. T. Fang and J.-G. Duh, Surface and Coatings Technology, 201, 1886 (2006).
- 35. Y. Furushima, C. Yanagisawa, T. Nakagawa, Y. Aoki and N. Muraki, *Journal of Power Sources*, **196**, 2260 (2011).
- 36. Y. Baba, S. Okada and J.-i. Yamaki, *Solid State Ionics*, **148**, 311 (2002).
- 37. J. Geder, H. E. Hoster, A. Jossen, J. Garche and D. Y. W. Yu, *Journal of Power Sources*, **257**, 286 (2014).
- 38. A. Basch, L. de Campo, J. H. Albering and J. W. White, *Journal of Solid State Chemistry*, **220**, 102 (2014).
- 39. E. Salagre, S. Quílez, R. de Benito, M. Jaafar, H. P. van der Meulen, E. Vasco, R. Cid, E. J.
- Fuller, A. A. Talin, P. Segovia, E. G. Michel and C. Polop, *Scientific Reports*, 11, 12027 (2021).
- 40. H. Wang, Y. I. Jang, B. Huang, D. R. Sadoway and Y. M. Chiang, *Journal of The Electrochemical Society*, **146**, 473 (1999).
- 41. A. R. C. Bredar, A. L. Chown, A. R. Burton and B. H. Farnum, *ACS Applied Energy Materials*, **3**, 66 (2020).
- 42. S. P. Rangarajan, Y. Barsukov and P. P. Mukherjee, *Journal of The Electrochemical Society*, **166**, A2131 (2019).
- 43. H.-W. Hsieh, C.-H. Wang, A.-F. Huang, W.-N. Su and B. J. Hwang, *Chemical Engineering Journal*, **418**, 129191 (2021).
- 44. R. Hausbrand, D. Becker and W. Jaegermann, *Progress in Solid State Chemistry*, **42**, 175 (2014).